Available online at www.sciencedirect.com
ScienceDirect
Journal of Magnetic Resonance 185 (2007) 191–203
JMR Journal of Magnetic Resonance
www.elsevier.com/locate/jmr

# Analysis of nitroxide spin label motion in a protein–protein complex using multiple frequency EPR spectroscopy

G.F. White [a], L. Ottignon [a], T. Georgiou [b], C. Kleanthous [c], G.R. Moore [a], A.J. Thomson [a], V.S. Oganesyan [a,*]

[a] School of Chemical Sciences and Pharmacy, University of East Anglia, Norwich NR4 7TJ, UK
[b] CCLRC Daresbury Laboratory, Warrington, Cheshire WA4 4AD, UK
[c] Department of Biology, University of York, York YO10 5YW, UK

Received 13 September 2006; revised 29 November 2006
Available online 16 December 2006

**Abstract**

X- and W-band EPR spectra, at room and low temperatures, are reported for nitroxide spin labels attached to cysteine residues selectively introduced into two proteins, the DNase domain of colicin-E9 and its immunity protein, Im9. The dynamics of each site of attachment on the individual proteins and in the tight DNase-Im9 complex have been analysed by computer simulations of the spectra using a model of Brownian dynamics trajectories for the spin label and protein. Ordering potentials have been introduced to describe mobility of labels restricted by the protein domain. Label mobility varies with position from completely immobilised, to motionally restricted and to freely rotating. Bi-modal dynamics of the spin label have been observed for several sites. We show that W-band spectra are particularly useful for detection of anisotropy of spin label motion. On complex formation significant changes are observed in the dynamics of labels at the binding interface region. This work reveals multi-frequency EPR as a sensitive and valuable tool for detecting conformational changes in protein structure and dynamics especially in protein–protein complexes.


*Keywords:* Colicin-E9; Computer simulation of EPR spectra; Electron Paramagnetic Resonance (EPR); Protein structure and dynamics

## 1. Introduction

The EPR spectra of nitroxide spin labels, selectively attached to specific amino acid residues, termed site-directed spin labelling (SDSL), has found a wide range of applications in the analysis of protein structure, function and dynamics. It has proved particularly useful for studies of high molecular weight proteins and membranous systems not always accessible to X-ray or NMR methods [1–6]. Three fundamental types of information can be obtained, the dynamics of the nitroxide label and its protein environment, the distance of the nitroxide from a second radical or bound paramagnetic metal ion and the accessibility of the label to collision with paramagnetic reagents in solution. Analysis of protein backbone dynamics and estimates of distances between selected sites on proteins can, however, be problematical because the spin label is invariably attached via a flexible linker to the protein [7–10].

In this paper we explore the use of a nitroxide label as a motional probe. Fig. 1 shows the attachment of the cysteine-specific nitroxide formed by reacting methane thiosulphonate reagent (MTSL) with the thiol side chain of cysteine, the label of choice for the majority of SDSL studies [11–13]. Spin label EPR spectra are sensitive to different types of molecular motion, which may be anisotropic and can include contributions from the flexibility of the label side-chain relative to the protein, rotary diffusion of the protein and, in some cases, local protein backbone fluctuations [10]. The motions of the spin label itself can be very complex and general dynamic models are needed to rationalise EPR data. An X-ray crystallography study has

* Corresponding author.
*E-mail address:* V.oganesyan@uea.ac.uk (V.S. Oganesyan).

1090-7807/$ - see front matter © 2006 Elsevier Inc. All rights reserved.
doi:10.1016/j.jmr.2006.12.009

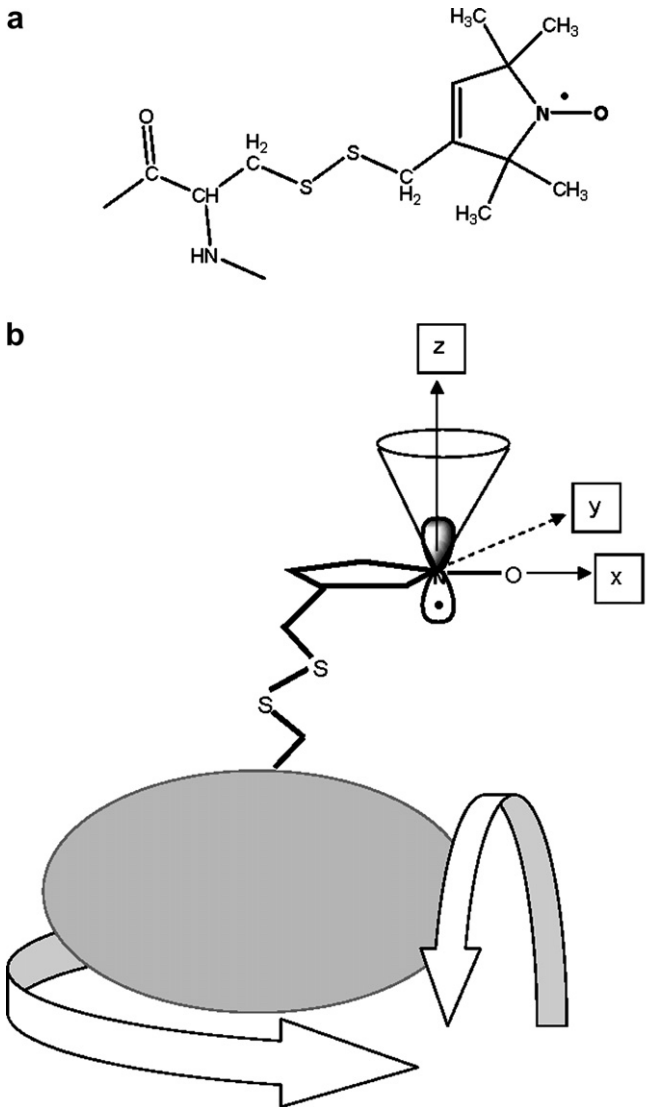


Fig. 1. Attachment of an MTSL side chain to a cysteine residue showing: (a) the molecular structure and (b) its relationship to the protein backbone defining the co-ordinates of the molecular axes system.

reported on the structures of MTSL labelled cysteine-containing variants of T4 lysozyme [14]. Different conformations of spin label were observed for some sites resulting from interactions between the nitroxide ring and its neighbouring protein residues. It was concluded that weak interactions between the disulphide attachment group and the protein backbone constrain the motion of the nitroxide side chain at surface sites. Therefore, at buried and tertiary contact sites, the MTSL side chain is able to access different conformations to minimise steric hindrance. In some cases, there was evidence in spin label EPR spectra for equilibria between two distinct conformations [3,15].

The aims of this study are to use X-band (9.5 GHz) and W-band (95 GHz) EPR to probe the motions of the spin label MTSL attached to different sites on the proteins colicin E9 DNase, its immunity protein Im9 and the protein–protein complex formed between them. Using computer spectral simulation we provide quantitative assignments relating to the local environment and mobility of the label and protein. We then apply the methods to observe changes that follow the formation of the protein–protein complex. Consideration of motional effects involves a variety of adjustable parameters and unique spectral simulations can be difficult to achieve, especially when the local protein environment limits the independent mobility of the label [16,17]. By using multiple EPR frequencies, spectra can be obtained that are sensitive to different time scales thus helping the de-convolution of the various motional contributions. The increasing availability of W-band (95 GHz) spectrometers are making this more common [15,18–20]. An alternative approach to this problem has been the addition of a thickening agent, often the polysucrose Ficoll, which is used to increase the solvent viscosity hence slowing down the rotary diffusion of the protein [21].

Colicin E9 DNase and its immunity protein, Im9, were chosen for this study because they are relatively small, water-soluble proteins, already well-characterised by NMR and X-ray crystallography [22,23]. Colicin E9 DNase is the cytotoxic domain of an endonuclease, colicin E9, produced by *Escherichia coli* to act against competing *Enterobacteria* [24,25]. Colicin-producing cells are protected against suicide by immunity proteins which specifically bind to, and inactivate, the cytotoxin [26]. Following receptor binding, the immunity protein, which in the case of the E9 DNase is Im9 [22,23], is thought to be released from the protein complex, allowing the cytotoxic domain to translocate into the target and initiate cell death [27]. Fig. 2 shows the crystal structure of the colicin E9 DNase-Im9 complex

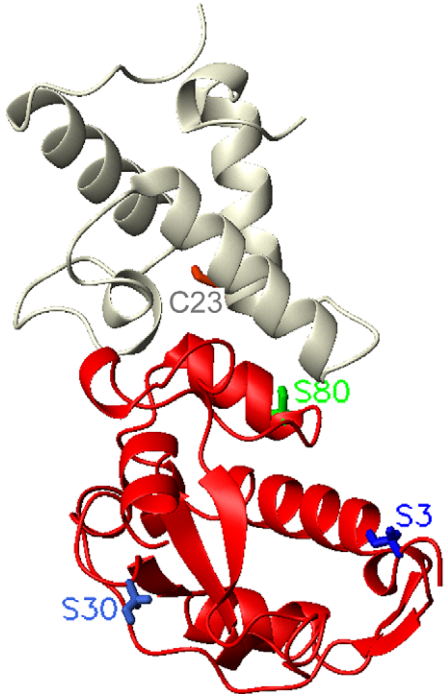


Fig. 2. Ribbon diagram showing the X-ray structure of Colicin E9 DNase (red) and Im9 (grey) complex (22). C23 of Im9 is marked. Serines 3, 30 and 80 are the sites of cysteine mutation in E9 DNase.

highlighting the sites selected for cysteine-specific spin label attachment, namely, S3, S30, S80 on E9 DNase and C23 on Im9. C23 is the only Cys residue on Im9 whereas E9 DNase is naturally Cys-free and it was necessary to prepare the variants S3C, S30C and S80C by site-directed mutagenesis. Studying the individual proteins and the protein–protein complex provided a variety of differently conformed sites for spin label attachment. These included sites at solvent-exposed, and protein-buried, α-helical regions, plus sites on a loop and an N-terminal strand. Once the sensitivity of SDSL has been established for conformational changes associated with these protein domains, the technique can be applied to the study of larger colicin systems and complexes with lower binding affinities that are difficult to study by other methods.

## 2. Materials and methods

### 2.1. Experimental techniques

#### 2.1.1. Materials

1-Oxyl-2,2,5,5-tetramethyl-$\Delta^3$-pyrroline-3-methyl (MTSL) was purchased from Toronto Research Chemicals, Canada. HEPES, CHELEX 100 and Dithiothreitol (DTT) were from Sigma-Aldrich, UK. De-salting columns filled with Sephadex G-25 (PD10 columns) were obtained from Amersham Biosciences, UK. The polysucrose, Ficoll 400, was purchased from Avocado Organics, UK.

#### 2.1.2. Expression and purification of Im9 and colicin E9 DNase cysteine variants

Im9 was prepared and purified as described by Wallis et al. [28]. Colicin E9 DNase variants S3C, S30C and S80C were constructed by site-directed mutagenesis and the proteins purified essentially as described previously [29]. Purified proteins were Amicon exchanged into 20 mM HEPES pH7 that had been de-ionised by passage over CHELEX 100 resin. Protein concentrations were determined by absorption at 280 nm using previously reported extinction coefficients: for Im9 $\varepsilon_{280} = 11{,}400\ M^{-1}\ cm^{-1}$; for E9 DNase $\varepsilon_{280} = 17{,}550\ M^{-1}\ cm^{-1}$[28,30].

#### 2.1.3. Spin labelling of colicin Im9 and E9 DNase variants

In order to ensure the reduction of any disulfides that may have formed, the E9 DNase variants were treated with DTT prior to spin labelling. This procedure was not necessary for Im9 as the natural Cys 23 residue is known not to crosslink. Treatment with DTT was carried out in an anaerobic glove box where 1 ml of DTT solution (1 mg/ml) was added to a 1.5 ml protein solution. After mixing, excess DTT was removed using a PD10 de-salting column. MTSL was stored at −80 °C as a 40 mM stock solution in acetonitrile. Small aliquots of MTSL stock were added to 2.5 ml protein solution to give a 4:1 label:protein ratio. The mixture was foil wrapped and incubated at room temperature for 4 h with gentle mixing. Excess spin label was removed by treatment with two successive PD10 columns followed by concentration using centrifuge-spun micro-concentrators. Protein concentration was determined by absorption at 280 nm and spin label concentration was checked by comparing the integrated EPR absorbance spectrum of a spin labelled protein with that of an MTSL standard. The degree of labelling was greater than 95% in every case. The purity of the spin labelled products was ascertained by mass determination using electrospray mass spectrometry. The molecular mass determined for purified Im9 was 9580 without label and 9765 with spin label attached. For the E9 DNase variants, the mass was 15,105 without label and 15,290 with spin label attached.

#### 2.1.4. Addition of polysucrose thickening agent

A stock solution of 60% w/w Ficoll 400 was prepared in 20 mM HEPES pH 7 buffer. This was used as the additive to prepare polysucrose thickened solutions of the spin labelled proteins.

#### 2.1.5. EPR spectroscopy

Room temperature X-band EPR spectra were acquired using a Bruker, EleXsys 500 spectrometer fitted with an ER4123D resonator with samples contained in 0.6 mm i.d. × 0.84 mm o.d. quartz tubes [31,32]. A Bruker EleXsys 580 system with an ER4118X-MD resonator was used in the continuous-wave mode to record X-band EPR at 170 K. For this system 3 mm i.d. × 4 mm o.d. quartz tubes were used. All W-band, EPR spectra were acquired using a Bruker, EleXsys 680 spectrometer with samples contained in 0.1mm i.d. × 0.5 mm o.d. quartz tubes.

## 3. EPR simulation of protein-bound spin labels undergoing motion

Currently, there are two general theoretical approaches to the simulation of the EPR of spin labels undergoing anisotropic motions with orientational constraints. First, the model developed by Freed and co-workers is based on the stochastic Liouville approach [16,33] and has been widely applied to study proteins, amorphous polymers and nucleic acids with remarkable success [6,15,35,36]. The advantage is the relative ease of simulation and analysis when simple forms of ordering potential, which can be expressed analytically, are considered. The second, described by Robinson et al. [34], is based on the simulation of EPR spectra from Brownian rotational diffusion trajectories of spin-label orientations which is more suitable for complex potential energy surfaces obtained say from Molecular Dynamics simulations [17]. This approach has been successfully used by Steinhoff and Hubbell for the simulation of X-band EPR spectra of a spin labelled polyleucine α-helix trimer [17].

Simulations of EPR spectra reported in this paper were performed using the module EPRSSP_DYN of an EPR computer simulation program developed in our laboratory. This procedure is based on a general method for the direct numerical simulation of CW EPR spectra of nitroxide spin

labels from Brownian rotational dynamics trajectories of protein and spin label orientations [34]. Our program considers the general case in which the overall spin label motion is the superposition of Brownian rotational diffusion of the protein and the independent motion of the spin label. These are described by two rotational diffusion tensors characterised by principle values and orientations. We have combined the Brownian dynamics approach with the introduction of ordering potentials for restricted mobility which are expressed using spherical harmonics. A motion in an axially symmetric potential along a single mode is associated with an order parameter $S$, calculated from the dynamical trajectories generated according to:

$$S = 1/2(3\langle\cos\beta^2\rangle - 1)$$

where $\beta$ is the angle between the $z$-axis of the spin label and the vector of the mode of the motion directed along the minima of a restricted potential in the protein domain. The average is taken over all dynamical trajectories and all points of time along the trajectory until the rotational correlation function relaxes.

In order to describe multi-modal dynamics of spin label we have introduced into our simulation program a so-called "hopping" model of the spin label. This assumes an additional slow component in the spin label motion due to transitions between localised modes described by forward and backward hopping rates between each pair of discrete rotameric states. In the case of only two modes of motion this model reduces to the two-jump problem (TJP) described in [34]. For ordered, or non-evenly distributed, samples each "jump" between a pair of states would require a unitary transformation of the spin label orientation described by a rotational matrix connecting the dirtections of two modes of motion within a protein domain. For randomly oriented molecules this operation is not necessary since all possible orientations relative to magnetic field are taken into consideration at each particular time step. In the "hopping" model the overall motion of the spin label becomes a superposition of the fast motion contribution, when the label explores the conformations about a central dynamic mode of restriction, and a slow motion, when spin label samples different modes. In order to obtain the evolution in time associated with the "jumps" between different states the dynamic Monte Carlo simulation algorithm has been applied [37].

## 4. Complementarity of X- and W-band EPR in the deconvolution of spin label and protein motions

The rotational diffusion of a moderate size protein on the EPR lineshape is significant [38]. Hubbell and co-workers have shown that in the case of an axially symmetric ordering potential along the nitroxide $z$-axis, the so-called microscopic order macroscopic disorder (MOMD) model, which is the equivalent of randomly distributed protein molecules with no motions present, was inadequate to reproduce EPR spectra at X-band of SL T4 lysozyme [15]. The slowly relaxing local structure (SRLS) model provided a much better fit. In their numerical and qualitative analysis of EPR spectra of a relatively small protein, neurotoxin, Timofeev and Tzvetlin have shown that the X-band spectra of five spin labelled derivatives recorded at different conditions are sensitive to the overall protein motion [38].

To illustrate the effect of protein rotational diffusion on the EPR spectra we have calculated spectra at X- and W-band for a variety of motional parameters using the simulation method described in the previous section. Fig. 3(a) shows the results at X-band (solid line) when the rotational diffusion of a protein molecule with an isotropic correlation time of $t_c = 7.5$ ns is taken into account assuming the spin label is rigidly bound compared with the simulation (dashed line) presenting the rigid limit. The dramatic difference between the two spectra shows that averaging of the shape of the first spectrum is caused by the motional contribution from the protein domain. Fig. 3(b) compares W-band spectral simulations using a range of protein rotational correlation times between 1 and 50 ns. The rigid limit at 95 GHz is attained for proteins with rotational diffusion correlation times longer than ~50 ns. In order to slow down the overall tumbling of the protein a thickening agent, such a w/w Ficoll 400 can be used [21]. The other way to separate motions is to measure EPR at different frequencies. Hyperfine interactions are intrinsic to the molecular environment of the paramagnetic moiety and are therefore independent of the applied magnetic field, thus giving the same frequency splittings at X-band and W-band. However, Zeeman interaction is field dependent and $g$-value anisotropy thus becomes more significant contribution to the W-band spectra. Fast motions average $g$-anisotropy at W-band in accordance with the condition: $\tau_i \leqslant \frac{1}{2}(v_0\Delta g_{ii} + 2.8\Delta A_{ii})^{-1}$, where $\tau_i$ is correlation time of rotational diffusion along the $i$-axis, $v_0$ is the resonance frequency of the EPR spectrometer and $\Delta g_{ii}$ and $\Delta A_{ii}$ (in Gauss) represents the deviation of the principle values from the average values of $g$ and $A$ tensors, respectively. Hence, W-band EPR line shapes are sensitive to a different dynamic range than X-band lineshapes. This is valuable in the analysis of spin label dynamics since slow motions that contribute to line shape changes at X-band are less likely to cause averaging effects in the W-band spectrum [15,19].

## 5. Results and discussion

In this section we present X- and W-band EPR spectra in frozen and liquid states of MTSL labelled E9 DNase variants S3C, S30C and S80C and C23 of Im9. Spectra were recorded for each spin labelled sample alone. In addition, samples were prepared containing equimolar spin labelled E9 DNase with non-labelled Im9 and vice versa, so that spin labelled sites on the on the E9-Im9 complex could be compared with those on individual proteins. Room temperature X-band EPR of labelled E9 DNase variants were also recorded in the presence of 30% Ficoll

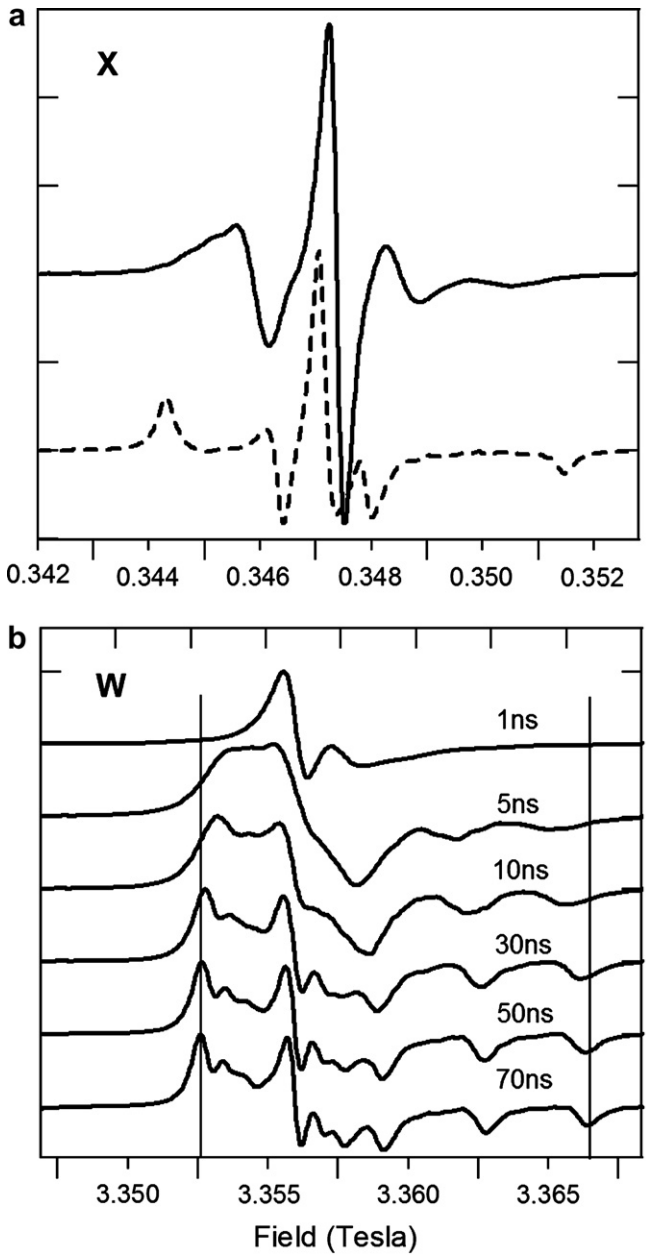


Fig. 3. Spectral simulation of the EPR spectra of a protein-bound nitroxide radical at X and W-bands undergoing rotational diffusion. (a) X-band. Solid line—isotropic rotational diffusion of a protein with an isotropic correlation time $\tau_c = 7.5$ ns. Dashed line—with no protein motion. The parameters describing the spin label motion are: $\tau_c(x) = \tau_c(y) = \tau_c(z) = 1$ ns and an order parameter $S = 0.87$ (see text). (b) W-band. Spectral simulations using a range of protein isotropic rotational correlation times as indicated. The spin label is taken to be rigidly bound to the protein molecule. Vertical lines represent the positions of the high and low field peaks in the spectrum under "rigid limit" conditions.

400. The spectra are not shown but the correlation times derived from the best-fitting simulations are given in Table 1. The motional parameters describing the dynamics of the spin label and protein are derived from the computer simulation described earlier. The effect of the formation of protein–protein complex on the changes of EPR line shapes for some of the sites of attachment has also been analysed.

### 5.1. Low temperature EPR spectra

X- and W-band EPR spectra of spin labelled Im9 and E9 DNase variants were recorded at 170 K, the temperature at which molecular motions, both label and protein, are frozen giving rigid limit spectra. The spectra were simulated, using a method developed by VSO, taking into account the random distribution of molecules in frozen solution at low temperature [39,40]. There is little variation between the spectral features of the nitroxide label as a function of points of attachment to the proteins at either frequency. Fig. 4 shows the spectrum of one spin labelled variant, E9 DNase S3C, with its simulation. Firstly, the magnetic parameters were adjusted manually in the spectral simulation to reproduce the main features of the experimental EPR spectra. Then a standard non-linear least-squares fitting routine was applied to minimise the RMS between theoretical and experimental points. The following parameters were derived for both colicin E9 and Im9: $g_{xx} = 2.0085$, $g_{yy} = 2.0063$, $g_{zz} = 2.0025$, $A_{xx} = 6.0$ G, $A_{yy} = 6.0$ G, $A_{zz} = 36.6$ G. At X-band the frozen solution spectrum is determined by the anisotropy of the hyperfine tensor. On the other hand, at W-band the hyperfine tensor is small compared to the anisotropy of the Zeeman interaction and all three principle components of the $g$-tensor are clearly resolved, each with its associated hyperfine splitting. The anisotropy of the hyperfine splitting arises because the $p_\pi$ orbital of the unpaired electron is asymmetric, making dipolar interactions between the electron and nucleus orientation dependent. The hyperfine interactions are stronger when the $z$-axis of the $p_\pi$ orbital is aligned with the magnetic field, $A_{zz}$, and weaker when the field is aligned perpendicular, $A_{xx}$ and $A_{yy}$. These values of the magnetic parameters of **g** and **A** tensors have been used in the simulation of room temperature EPR spectra.

### 5.2. Room temperature EPR spectra

#### 5.2.1. Colicin E9 DNase variants S3C and S80C

Room temperature EPR spectra at both X- and W-band reveal fast, unconstrained motion of the spin label on variants S3C and S80C of the E9-DNase, Fig. 5(a) and (b) and S2 of Supporting information, respectively. As shown in Table 1, successful simulations at both frequencies require only a single isotropic rotation of $\tau_c = 0.46$ ns and $\tau_c = 1.15$ ns, respectively, for S3C and S80C arising from the motion of the label. Because of the fast and unrestrained motion of the spin label relative to the protein neither the X- or W-band spectra appear sensitive to the overall motion of the protein. Indeed, the spectra calculated from spin-only rotational diffusion dynamics were indistinguishable from spectra that included the dynamics of the E9-DNase protein. Note that our computer model is able to reproduce all the essential features of the EPR spectra

Table 1
Parameters of protein and label dynamics from the simulation of room temperature EPR spectra of MTSL labelled colicin E9 DNase, Im9 and the E9-Im9 complex

| Site (protein) | Component | | $\tau_c(x)$ (ns) label | $\tau_c(y)$ (ns) label | $\tau_c(z)$ (ns) label | $S$[a] | $\tau_c$ (ns) protein | $T_2$ X-band (μs) | $T_2$ W-band (μs) | $\chi^2$[b] |
|---|---|---|---|---|---|---|---|---|---|---|
| S3C (E9) | 1 | | 0.46 | 0.46 | 0.46 | 0 | — | 0.0467 | 0.0260 | 0.0386 |
| | | | | | | | | | | 0.0687 |
| S3C (E9-Im9) | 1 | | 0.46 | 0.46 | 0.46 | 0 | — | 0.0467 | 0.0260 | 0.0344 |
| | | | | | | | | | | 0.0666 |
| S80C (E9) | 1 | | 1.15 | 1.15 | 1.15 | 0 | 7.7 | 0.0362 | 0.0260 | 0.0358 |
| | | | | | | | | | | 0.0669 |
| S80C(E9-Im9) | 1 | 50% | 0.83 | 0.83 | 0.83 | 0.85 | 9.5 | 0.0304 | 0.0270 | 0.0654 |
| | 2 | 50% | — | — | — | 1 | 9.5 | 0.0322 | 0.0304 | 0.1413 |
| S30C (E9) | 1 | 40% | 1.15 | 1.15 | 1.15 | 0 | 7.7 | 0.0210 | 0.0255 | 0.0648 |
| | 2 | 60% | — | — | — | 1 | 7.7 | 0.0303 | 0.0255 | 0.0776 |
| S30C (E9-Im9) | 1 | 40% | 1.15 | 1.15 | 1.15 | 0 | 9.5 | 0.0210 | 0.0255 | 0.0459 |
| | 2 | 60% | — | — | — | 1 | 9.5 | 0.0303 | 0.0255 | 0.0788 |
| C23 (Im9) | 1 | | 0.40 | 11 | 11 | 0 | 4.8 | 0.0304 | 0.0397 | 0.0390 |
| | | | | | | | | | | 0.0852 |
| C23 (E9-Im9) | 1 | 25% | 1.15 | 1.15 | 1.15 | 0 | 9.5 | 0.0210 | 0.0255 | 0.0432 |
| | 2 | 75% | — | — | — | 1 | 9.5 | 0.0303 | 0.0255 | 0.0777 |
| S3C (E9) 30% ficoll | 1 | | 0.60 | 0.60 | 0.60 | 0 | — | 0.0467 | 0.0260 | 0.0340 |
| | | | | | | | | | | 0.0700 |
| S80C (E9) 30% ficoll | 1 | | 1.66 | 1.66 | 1.66 | 0 | — | 0.0362 | 0.0260 | 0.0378 |
| | | | | | | | | | | 0.0650 |
| C23 (Im9) 30% ficoll | 1 | | 0.52 | 14.4 | 14.4 | 0 | — | 0.0467 | 0.0260 | 0.0391 |
| | | | | | | | | | | 0.0630 |

[a] $S = 0$ and $S = 1$ correspond to completely unrestricted (no ordering potential) and rigidly bound states of spin label, respectively.
[b] Standard deviations between simulated and experimental spectra at X- and W-band, respectively.

using a minimal set of adjustable parameters. For the sake of simplicity, the bandwidth defined by the transverse relaxation time $T_2$ is assumed to be isotropic and independent of hyperfine coupling. This assumption reduces the number of adjustable parameters required to achieve satisfactory fits of experimental spectra. Although improved fits could be achieved by variation of bandwidth parameters, this would not add extra information. In order to display the quality of the simulated spectra a standard deviation function could be introduced. However, in the majority of cases applications of least-square fitting routines to EPR spectra results in improvement to the deviation factor at the cost of losing the essential characteristic features of the spectrum. Therefore, our strategy was first to achieve a reasonable fit of each X-band EPR spectrum by eye and then, where appropriate, to perform additional least-squares optimisation. We have found that, in most cases, the accuracy estimated by eye was satisfactory. The calculated standard deviations for each spectrum are included in Table 1.

It is reported that for molecular weights $\leqslant$15 kDa protein tumbling motions may contribute to motional averaging effects observed in X-band EPR of spin labels [3]. Colicin E9 DNase and Im9 fall within this range. The rotational correlation times for colicin E9 DNase, Im9 and the complex formed between them, estimated from time resolved fluorescence and anisotropy decay analysis, are $\tau_c = 8.6$ ns for colicin E9 DNase, $\tau_c = 2.69$ ns for Im9 and $\tau_c = 14.0$ ns for the E9-Im9 complex [41]. For spin labels attached at sites 3 and 80 on E9 DNase, contributions from these motions must be slow compared with the correlation times of the unrestricted spin label so that the spin label motions are the origin of the averaging effects observed in both X- and W-band EPR.

X-band room temperature EPR experiments were also carried out with spin labelled S3C and S80C variants dissolved in 30% Ficoll 400. The correlation times derived from X-band spectral simulations were $\tau_c = 0.60$ ns and $\tau_c = 1.66$ ns, respectively. The increase in viscosity has slowed the spin label motions by factors of 1.3 and 1.4. If overall protein tumbling were contributing to the spin label dynamics, the slowing factor should be closer to 3 [21]. This indicates that the spin label motions must be restrained, to a small degree, by interactions with the protein but largely, it has the freedom to move independently of the protein [10,21]. Combining knowledge of the protein structure with evidence from the spin label EPR experiments, it can be assumed that the X-band EPR line shape observed for spin labelled E9 DNase S80C is typical for MTSL attached to the solvent-exposed surface of an α-helix. The fact that the effective correlation time appears faster for the spin label on S3C, almost by the factor of 2, is due to its position on a flexible N-terminal strand.

### 5.2.2. Colicin E9 DNase variant S30C

The room temperature EPR spectra of spin labelled E9 DNase S30C, Fig. 6, present quite different results to those of the variants S3C and S80C. The most distinctive features are the observation, at X-band, of both a broad signal, signifying slow and restricted spin label dynamics, and

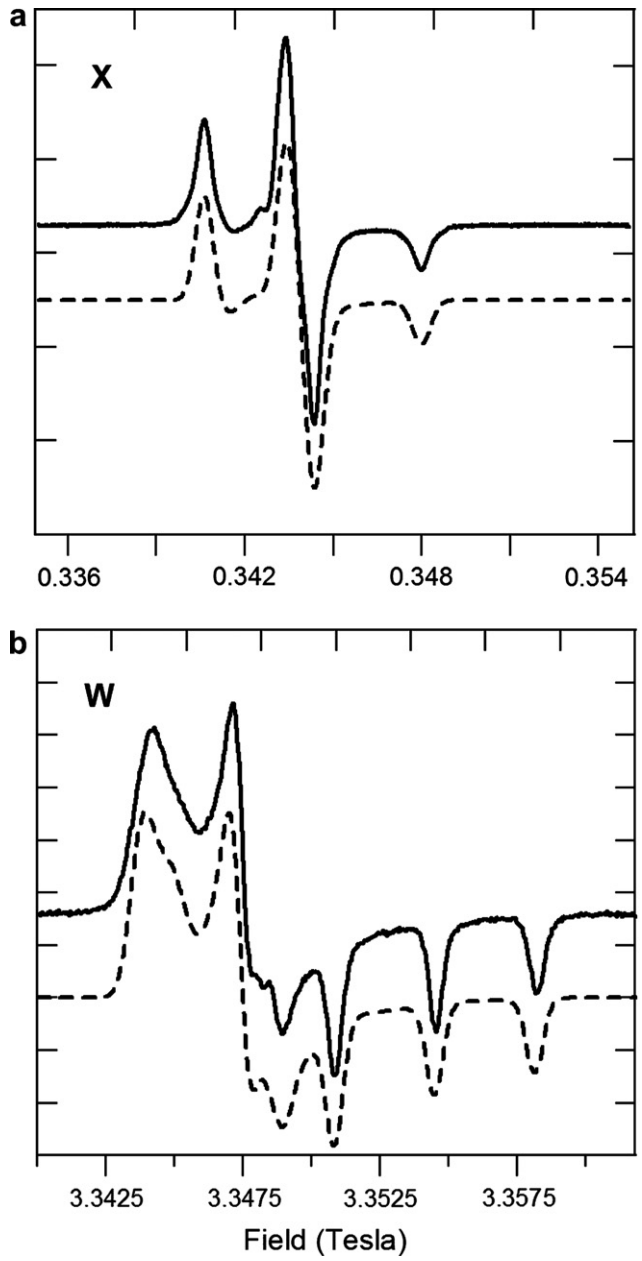


Fig. 4. Experimental (solid line) and simulated (dashed line) EPR spectra of MTSL label on colicin E9 DNase S3C recorded at 170 K. Experimental conditions: Concentration of MTSL = 200 μM, Spectra recorded at (a) X-band, frequency = 9.7 GHz, power = 2.0 mW, modulation amplitude = 1 G; (b) W-band, frequency = 94.2 GHz, power = 0.45 μW, modulation amplitude = 1 G. Parameters used in the simulation of EPR spectra are given in the text.

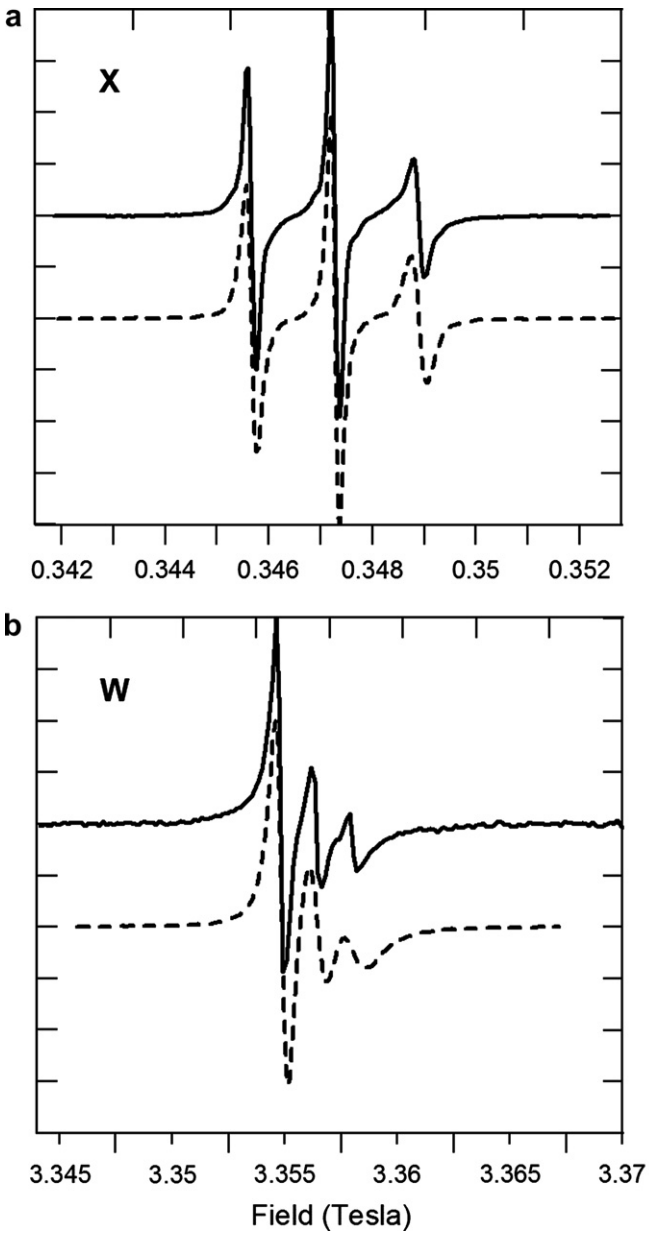


Fig. 5. Experimental (solid line) and simulated (dashed line) room temperature EPR spectra of MTSL attached to S3C on E9 Dnase. (a) X- and (b) W-band. Experimental spectra were recorded under the following conditions: X-band: concentration: 200 μM, frequency = 9.7 GHz, power = 2.0 mW, modulation amplitude = 1 G, temperature = 295 K. W-band: concentration was 500–600 μM, frequency = 94.2 GHz, power = 0.113 mW, modulation amplitude = 1 G. Simulations of spectra have been performed using parameters shown in Table 1. Upon addition of Im9 to E9 no changes are observed in the EPR spectra (data not shown).

narrower central features, associated with faster motions. The latter, sharper peaks match the positions of the three hyperfine lines observed in the fast motional regime. Using a two component model a satisfactory fit can be achieved. Analysis suggests that 40% of the spin label undergoes free rotational dynamics described by the following set of parameters; a correlation time of $\tau_c = 1.15$ ns for the label and $\tau_c = 7.7$ ns for the protein, while 60% of the label is in a rigidly bound state with $\tau_c = 7.7$ ns for the protein (see Table 1). The hopping rates between the two modes of motion used in the simulation for all sites experiencing bi-modal dynamics were too slow ($<10^7\ s^{-1}$) to affect the EPR lineshapes which manifest themselves as the sums of the independent contributions from two modes. The plateau observed at 3580G in the first derivative X-band spectrum, Fig. 6(a), is due to the superposition of the positive intensity of the fast motional component and the negative intensity contributed by the slow motion. Because of the

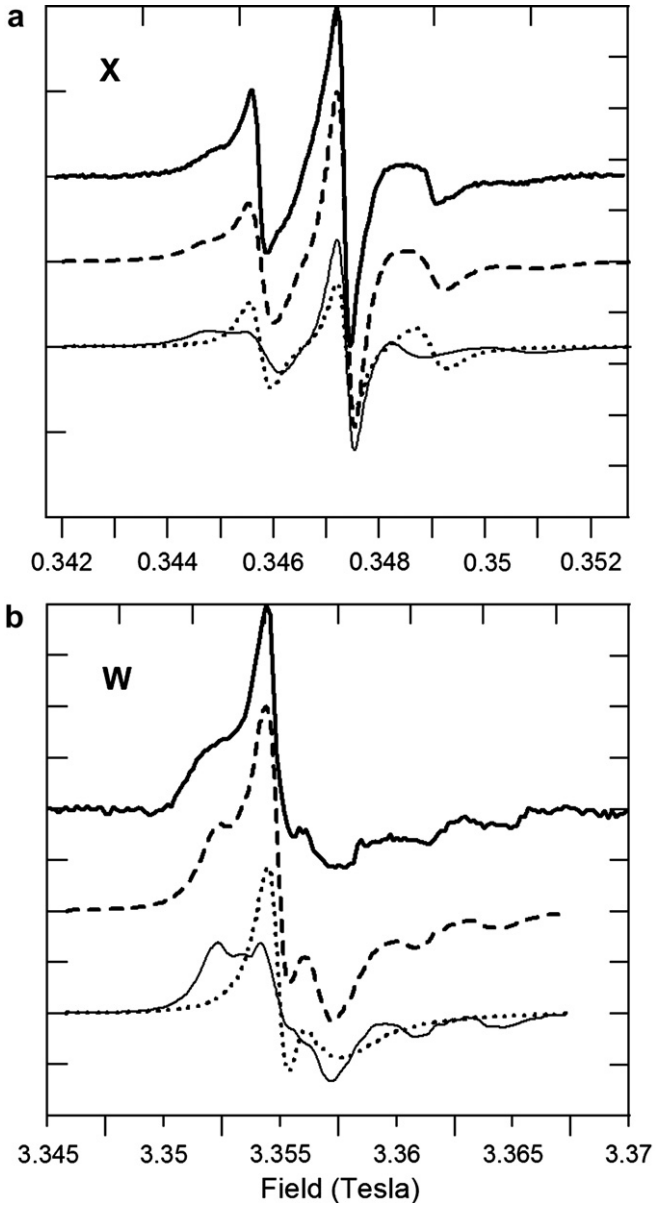


Fig. 6. Experimental (thick solid line) and simulated (dashed line) room temperature EPR spectra of MTSL attached at S30C on E9 DNase. (a) X- and (b) W-band. For experimental conditions see legend to Fig. 5. Simulations have been performed using parameters shown in Table 1. Contributions to EPR spectra from two conformations of the spin label are shown by dotted and thin solid lines for components 1 and 2, respectively (see Table 1).

substantial contribution from the spin label with restricted mobility, an accurate estimate of the protein rotational correlation time can be achieved. The parameters obtained from fitting the X-band spectrum have then been used to predict the W-band spectrum. Excellent agreement with the experimental spectrum is achieved (Fig. 6 (b)). The contributions from two components are even more apparent in the W-band spectrum. At 94 GHz, the spectrum contains both a motionally averaged narrow, intense band close to the centre of the spectrum with distinct $g_{xx}$ and $g_{zz}$ features with hyperfine splittings typical of a slow spin label. Comparison of Fig. 6(b) and Fig. 4(b) shows that the slow component of the spin label has not reached the rigid limit at W-band and hence the correlation time of the protein rotational diffusion can be estimated from the simulations of the averaging effects at X- and W-band.

### 5.2.3. Im9 C23

The room temperature X-band spectrum of spin label on Im9 C23, Fig. 7(a) is similar to those observed for high mobility sites where the spin label experiences no interactions with any protein side-chains, such as S80C on E9 DNase. Indeed, the spectrum can be fitted well without

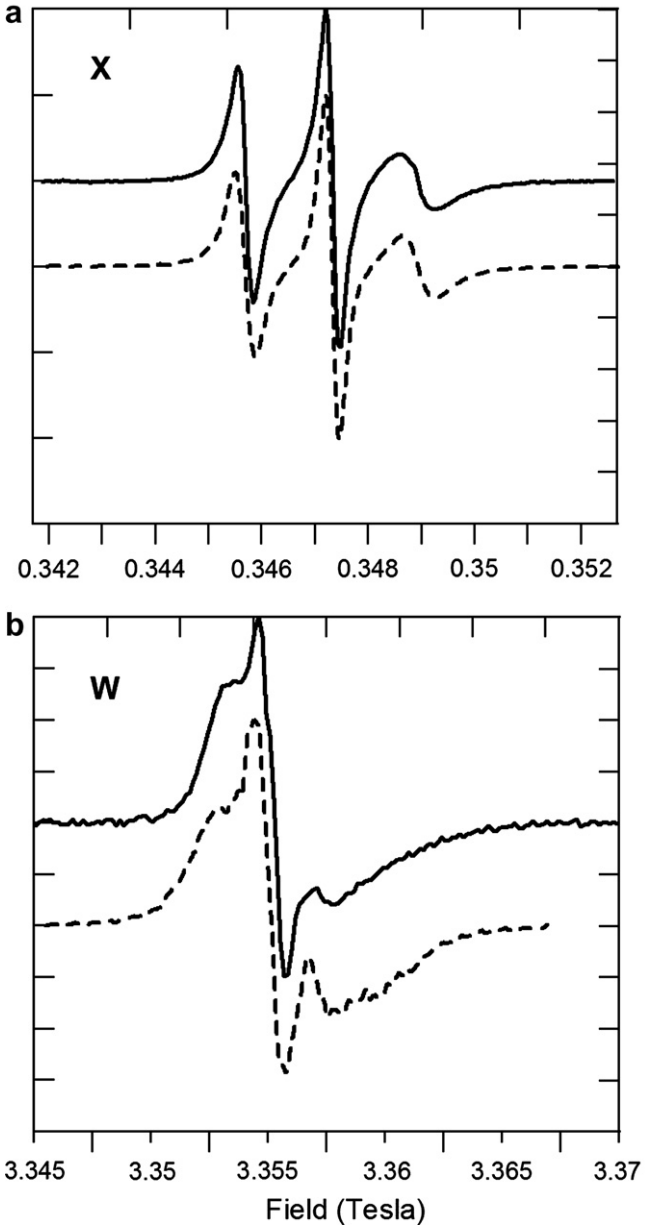


Fig. 7. Experimental (solid line) and simulated (dashed line) room temperature EPR spectra of MTSL attached at C23 site of Im9. (a) X- and (b) W-band. For experimental conditions see Fig. 5. Simulations of spectra have been performed using parameters shown in Table 1.

including the dynamics of the protein and using only an isotropic rotational diffusion with a correlation time $\tau_c = 1.62$ ns. This result was backed up by a Ficoll experiment carried out at X-band where, in the presence of 30% Ficoll 400, a good fit was achieved using an isotropic correlation time of $\tau_c = 2.1$ ns. This corresponds to a slowing factor of 1.3 which is the same as that found for all the sites on colicin E9 DNase.

However, the shape of the W-band spectrum, Fig. 7(b), is strikingly different from those observed for spin labels on E9 DNase, such as sites S80C and S30C, Figs. S1(b) and 6(b), respectively. For the spin label on Im9 C23, the $g_{xx}$ and $g_{yy}$ magnetic features are not completely averaged although the $g_{xx}$ and $g_{zz}$ signals are. At W-band the $g_{ii}$ and $g_{jj}$ features are only averaged if the frequency of rotation along the axis in the direction perpendicular is fast compared with $(g_{ii} - g_{jj})\beta B\hbar^{-1} \approx 8 \times 10^8\ s^{-1}$. The W-band spectrum of spin labelled Im9 C23 is a direct indication of anisotropic rotational motion of the spin label. Similar effects have been observed previously in the literature [19,42] The spectral shape can be explained if, on the W-band timescale, motional averaging in the $xz$ plane of the spin label is much faster than in both the $xy$ and $zy$ planes, that is, the rotation along the $y$ axis is the fastest. Using the model of axially symmetric anisotropic mobility of spin label we have been able to reproduce the spectral features of the W-band spectrum (Fig. 7(b)). A good fit was also achieved when the same parameters (shown in Table 1) were used to simulate the X-band spectrum (Fig. 7(a)). Although the X-band spectrum can be fitted equally well using either isotropic or anisotropic rotational diffusion models the W-band EPR spectrum clearly shows the anisotropic rotation which presumably arises from constraints imposed by the protein local structure. Our analysis shows that, because the spin label motion is highly anisotropic, the spectrum at W-band is also sensitive to the overall protein diffusional dynamics. Computer simulations reveal that protein motions with correlation times shorter than 4.8 ns would average out the anisotropy of $g_{xx}$ and $g_{yy}$.

### 5.2.4. Spectra of the E9 DNase-Im9 complex

EPR spectra have been recorded of the tight complex between E9 DNase and Im9 singly labelled at E9 DNase sites S3C, S30C, S80C and the Im9 site C23. These spectra are compared to those of spin labels on the individual proteins. Changes are anticipated due to the increase in the protein mass giving a slower overall tumbling time and possibly in label motions, especially those located in, or close to, the binding interface face region. For S3C, there were no differences between the spectra. Slight changes were observed in the spectra of the S30C site. Simulation shows they correspond to an increase of the protein rotational diffusion correlation time due to the increased protein mass (Fig. S2 of the Supporting information). The spectrum still does not fit a single dynamic simulation. Interestingly, the spectral line shape is similar to that obtained for spin labelled E9 DNase S30C with 30% Ficoll 400 added. This confirms that a slow down in rotary diffusion of the protein is influencing the EPR of the spin label on the protein complex in this case.

The situation is markedly different for the spin label on the S80C variant of E9 DNase complexed with unlabelled Im9. Fig. 8(a) and Fig. S1(a) compare the spectra of the complexed and uncomplexed proteins at X-band and Fig. 8(b) and Fig. S1(b) at W-band. The X-band spectra are characterised by wide asymmetric shapes for $I = \pm 1$

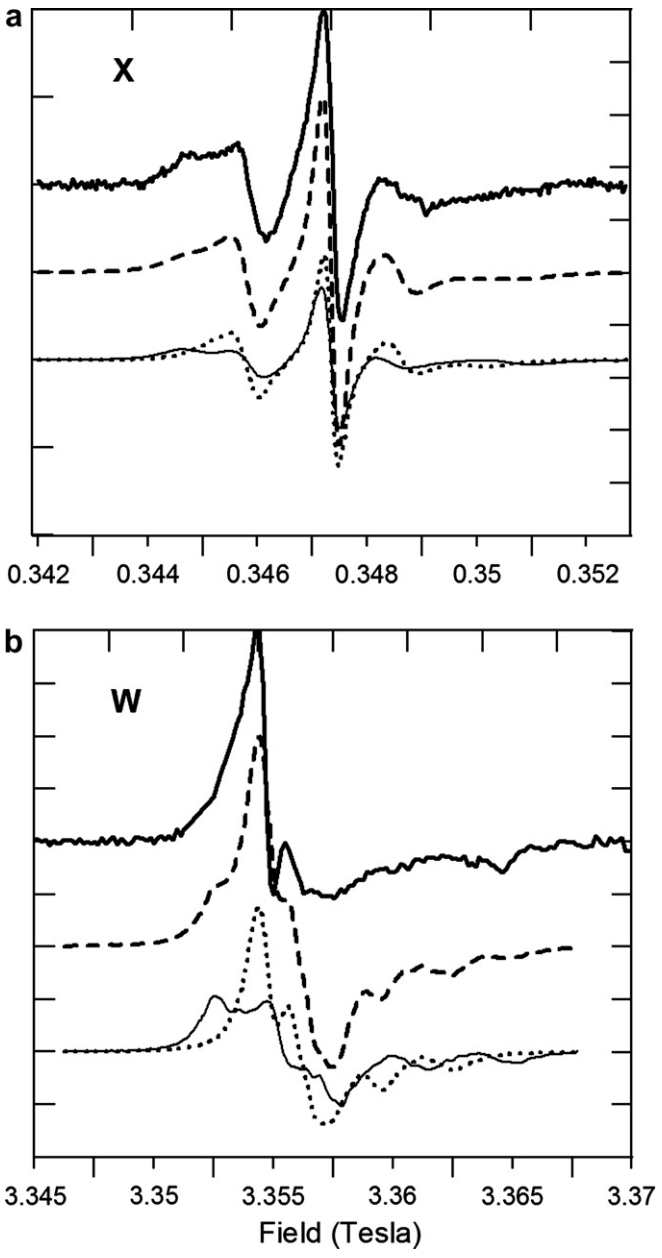


Fig. 8. Experimental (thick solid line) and simulated (dashed line) room temperature EPR spectra of MTSL on S80C in the E9 Dnase-Im9 complex. (a) X- and (b) W-band. For experimental conditions see Fig. 5. Spectral simulations have been carried out using parameters shown in Table 1. Contributions to EPR spectra from two conformations of the spin label are shown by dotted and thin solid lines for components 1 and 2, respectively (see Table 1).

hyperfine lines showing an increased restriction on the mobility of the label. The shapes are close to those of a single mode of motion with an axially symmetric restricting potential directed along the z- axis characterised by the order parameter, $S$ [10]. However, simulation with only one mode of Brownian motion does not reproduce an outer right peak in the spectrum and a second mode of motion with a higher degree of restriction of spin label mobility is required. The parameters of both components of motion contributing to the spectrum are given in Table 1. In fact, the slower component is well described by the model of a spin label rigidly bound to the protein complex ($S = 1$). In this case the overall dynamics of this mode depends only on the rotational diffusion constant of the E9-Im9 complex. Both components are shown in Fig. 8(a). The slow motional component is also apparent in the W-band spectra (Fig. 8(b)). Therefore, we conclude that, upon formation of the protein complex with Im9, the overall motion of the C80 label becomes significantly restricted consisting of two distinct components, namely, 75% fast but axially restricted motion along the $z$-axis and 25% in which the spin label is rigidly bound to a protein.

Note that although our model is able to reproduce the main features in EPR spectra some descrepancies between experimental and theoretical spectra exist, especially in some of the W-band spectra predicted from the parameters adjusted from the fittings of X-band spectra. As mentioned previously the simulation could be substantially improved by introducing additional parameters describing linewidths. This, however, would not provide extra information. This conclusion is valid for the X- and W-band EPR spectra of all the sites of attachment except the W-band spectrum of spin label on S80C in the protein–protein complex (Fig. 8(b)). Our simulations, which also have included non-collinearity of magnetic and rotational diffusion tensors of spin label, indicate that the dynamics of spin label at this position is more complex than the one described by axial ordering potential.

The X-band EPR spectrum of spin labelled Im9 C23 is also markedly different in the complex, see Fig. 9(a), and resembles that of spin labelled S30C in the E9-Im9 complex. An excellent fit can be achieved using the two component model with the parameters listed in the Table 1. The values obtained for motional parameters in the case of spin labelled Im9 C23 are similar to those of the E9 DNase S30C site except that the amount of the fast component in the spectrum is reduced to 25%. These parameters have been used to predict the W-band spectrum and are in excellent agreement with the experiment (Fig. 9(b)). The spectra of both the E9DNase S80C and Im 9 C23 labels have a component showing a spin label rigidly bound to the protein. The contribution of this motional mode is different being 50% for E9 DNase S80C and 75% for Im 9 C23, respectively. The anisotropic nature of the other mode of the spin label is different for each site. The label on Im9 C23 is unrestricted, whereas that on E9 DNase S80C is restricted along its $x$- and $y$-axis. This shows that in the complex, both labels on Im9 C23 and E9 DNase S80C can adopt two conformations.

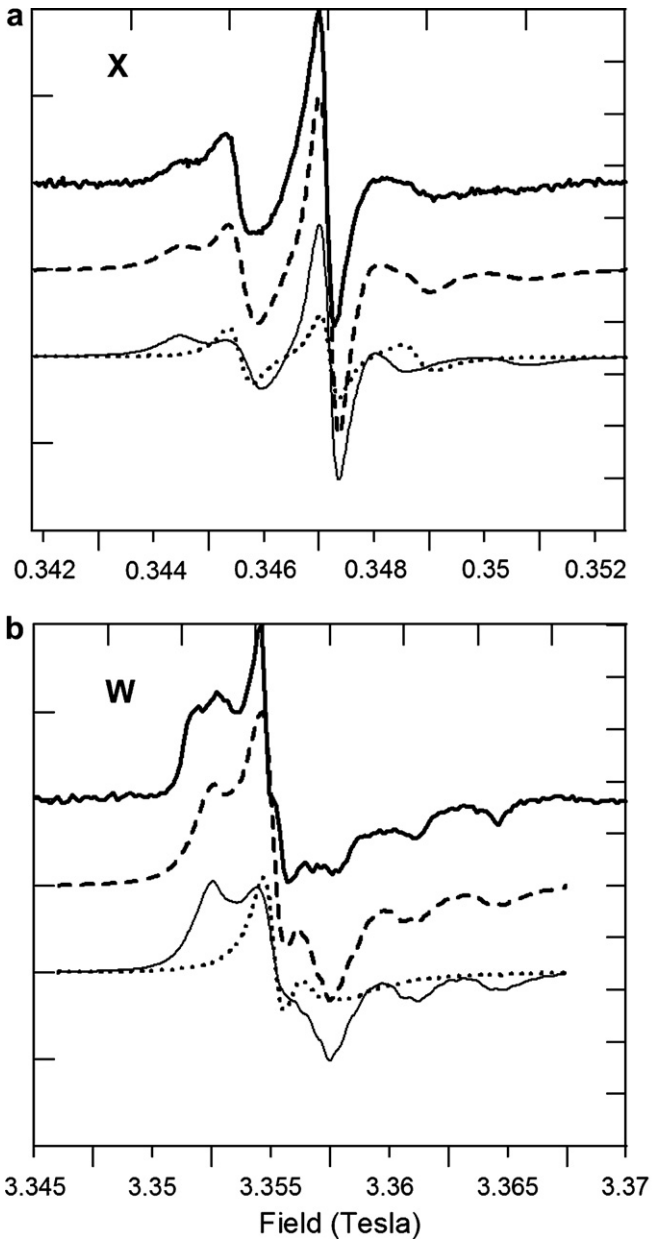


Fig. 9. Experimental (thick solid line) and simulated (dashed line) room temperature EPR spectra of MTSL on C23 on Im9 in the E9Dnase-Im9 protein complex. (a) X- and (b) W-band. For experimental conditions see Fig. 5. Simulations of spectra have been performed using parameters shown in Table 1. Contributions to EPR spectra from two conformations of the spin label are shown by dotted and thin solid lines for components 1 and 2, respectively (see Table 1).

### 5.3. Structural interpretations from the spin label dynamics

This will begin with a discussion of the results observed for spin labels on the individual proteins, followed by consideration of changes observed on formation of the E9 DNase-Im9 complex.

Although the EPR indicates that spin labels on sites S3 and S80 both have unrestricted surface motions, there is a significant difference between the determined correlation times. The serine residue at position 3 is solvent-exposed on an un-structured protein strand near the N-terminus whereas, S80, also solvent-exposed, lies at the end of the α-helix running from Asn72 to Lys81. For S3, NMR relaxation studies show the N-terminal strand experiences local backbone fluctuations that are fast compared to the rest of the protein [43]. For S80, NMR relaxation values match the average observed across the protein backbone and local backbone fluctuations are not expected to contribute to spin label mobility at this site [43]. Therefore, for a spin label on the S3C variant, it is likely that two factors contribute to the faster, isotropic motion observed in the EPR. The spin label experiences no interactions with any protein side-chains, only with solvent, and is attached to a region of protein that also exhibits local backbone fluctuations faster than, and independent from, the overall rotary diffusion of the protein.

The EPR of a spin label on S30C shows two independent motions having two different correlation times, one fast and one slow. The observation of independent conformations, such as this, is not uncommon in spin label EPR and is usually seen where the motion of the side chain is partially restricted but is less likely if the motion is either highly restricted or very mobile [14,15]. This interpretation fits well since S30C is near the surface of the protein on an unstructured loop where interactions with other parts of the protein are possible. The fact that the rotational diffusion tensor is anisotropic for spin labelled Im9 compared to spin labelled E9 DNase S80C indicates that there are interactions with neighbouring protein residues that restrict the surface motion in the *xy* and *zy* planes of the spin label side chain. The structure of the Im9 protein shows that C23 lies at the end of the α-helix running from Glu12 to Asn24. Although it is near the surface, this section of the helix faces other parts of the protein structure thus bringing the spin label side chain into closer contact with surrounding protein compared with S80C on E9 DNase.

It is clear from the X-ray structure, Fig. 2, that sites S3C and S30C on the E9 DNase are not close to the binding interface in the complex formed with Im9. This is borne out by the spin label EPR spectra that were acquired for the spin labels on the DNase alone and on the complex. The spectra of spin label on S3C are identical and the slight changes observed for the S30C site can be accounted for in terms of the slower tumbling rate of the complex (24.5 kDa) compared to the isolated E9 DNase (15 kDa). These results verify that a spin label attached at S3C rotates freely and has motion independent of the protein tumbling rate. NMR experiments have also shown no dynamic or structural changes at position S3C on complex formation [44].

In contrast, for sites S80C on E9 DNase and C23 on Im9 the spin label EPR spectra recorded for the protein–protein complex, Figs. 8 and 9, are different from those of the isolated proteins. In both cases, two distinct spin label motions are required to fit the spectral line shapes observed for the complex, each showing one more mobile and one rigidly bound component. The X-ray structure shows that both sites are situated in or close to the protein–protein binding interface and, therefore, in agreement with the EPR results, spin labels are more likely to be buried in the protein structure rather than surface exposed as they are in the isolated proteins [28]. In the case of Im9 C23 the more mobile mode (25%) is unrestricted, indicating that the spin label may adopt a conformation that is solvent exposed, whereas the fast component of the label on E9 DNase S80C (50%) shows axial restriction. This latter type of motion has been identified previously as characteristic of a label folded back against the protein backbone and likely to occur for a spin label at a buried helix site with tertiary contacts [10].

## 6. Conclusions

These results show that spin label mobility varies substantially with position within colicin E9 DNase and Im9, from completely immobilised, to a motionally restricted label and to free rotation. We have been able to derive information about the dynamics of each site of attachment within the protein E9 DNase and its complex with Im9 by performing computer simulation of EPR spectra at X- and W-band frequencies using the model of Brownian dynamics trajectories for the spin label and protein and by introducing ordering potentials to describe restricted mobility of spin label within the protein domain. The restricted mobility of spin label for most of the sites is fairly well described by an axially symmetric potential except for spin label on the S80C (E9-Im9) site (Fig. 8b) which shows more complex dynamics.

Both X- and W-band EPR spectra are sensitive to the overall protein rotational correlation times in cases where the spin label mobility is either substantially restricted or highly anisotropic (sites S30 (E9), C23 (Im9), S80C (E9-Im9), C23 (E9-Im9), S30C (E9-Im9); Figs. 6–9 and S2 of Supporting information, respectively). In this case the estimation of protein rotational diffusion correlation time is possible. On the other hand, X-band spectra are not particularly sensitive to the anisotropy of spin label rotation. In some instances they can be fitted equally well using either isotropic or anisotropic models. In contrast at W-band we have shown that accurate measurement of anisotropy of spin label motion is possible (Fig. 7b for C23 (Im9)).

Our computer simulation and analysis of EPR spectra show that, particularly in the protein–protein complex, those spin label sites at the binding interface region express bi-modal dynamics with one component being in the "buried" state and the other highly mobile and, therefore, solvent exposed (sites S30 (E9), S80C (E9-Im9), C23 (E9-Im9), S30C (E9-Im9); Figs. 6,8,9 and S2 of Supporting information, respectively). The hopping rates between two states of motion are sufficiently slow on both X- and

W-band EPR timescales to be quantified from the simulated spectral lineshapes.

Upon complex formation significant changes are observed at both X- and W- bands for those sites which are involved in the tertiary contacts between the two protein domains (sites C23 on Im9 and S80C on E9 DNase). Quantitative analysis using computer simulation provides rationalisation of these changes in terms of protein structure and dynamics. This reveals multi-frequency EPR spectroscopy as a sensitive tool for monitoring conformational transitions and changes in protein structure and dynamics particularly during formation of protein complexes.

## Acknowledgments

A.J.T. acknowledges support from BBSRC Grants 83/B17596 and BBS/B/03637 and from the Wellcome Trust for the award of equipment from the Joint Infrastructure fund. V.S.O. thanks the EPSRC for an Advanced Fellowship.

## Appendix A. Supplementary data

Supplementary data associated with this article can be found, in the online version, at doi:10.1016/j.jmr.2006.12.009.

## References

[1] W.L. Hubbell, H.S. Machaourab, C. Altenbach, M.A. Lietzow, Watching proteins move using site-directed spin labelling, Structure 4 (1996) 779–793.
[2] W.L. Hubbell, A. Gross, R. Langen, M.A. Lietzow, Recent advances in site-directed spin labelling of proteins, Curr. Opin. Struct. Biol. 8 (1998) 649–656.
[3] W.L. Hubbell, D.S. Cafiso, C. Altenbach, Identifying conformational changes with site-directed spin labelling, Nat. Struct. Biol. 7 (2000) 735–739.
[4] W.L. Hubbell, C. Altenbach, Investigation of structure and dynamics in membrane proteins using site-directed spin labelling, Curr. Opin. Struct. Biol. 4 (1994) 566–573.
[5] J. Torres, T.J. Stevens, M. Samso, Membrane proteins: the wild west of structural biology, Trends Biochem. Sci. 28 (2003) 137–144.
[6] P.P. Borbat, A.J. Costa-Filho, K.A. Earle, J.K. Moscicki, J.H. Freed, Electron spin resonance in studies of membranes and proteins, Science 291 (2001) 266–269.
[7] H.-J. Steinhoff, N. Radzwill, W. Thevis, V. Lenz, D. Brandenburg, A. Anston, G. Dodson, A. Wollmer, Determination of interspin distances between spin labels attached to insulin: comparison of electron paramagnetic resonance data with the X-ray structure, Biophys. J. 73 (1997) 3287–3298.
[8] M. Persson, J.R. Harbridge, P. Hammarstrom, R. Mitri, L-G. Martensson, U. Carlsson, G.R. Eaton, S.S. Eaton, Comparison of electon paramagnetic resonance methods to determine distances between spin labels on human carbonic anhydrase II, Biophys. J. 80 (2001) 2886–2897.
[9] G. Radzwill, H.-J. Steinhoff, Time-resolved detection of transient movement of helices F and G in doubly spin-labeled bacteriorhodopsin, Biophys. J. 80 (2001) 2856–2866.
[10] L. Columbus, W.L. Hubbell, A new spin on protein dynamics, Trends Biochem. Sci. 27 (2002) 288–295.
[11] L.J. Berliner, The spin label approach to labelling membrane protein sulfhydryl groups, Ann. NY Acad. Sci. (1983) 153–161.
[12] W.L. Hubbell, C. Altenbach, Site-directed spin labelling of membrane proteins, in: S.H. White (Ed.), Site-directed Spin Labelling of Membrane Proteins, Oxford University Press, 1994, pp. 224–247.
[13] L.J. Berliner, Spin Labeling: The Next MillenniumBiological Magnetic Resonance, vol. 14, Plenum Press, New York, 1998.
[14] R. Langen, K.J. Oh, D. Cascio, W.L. Hubbell, Crystal structures of spin labelled T4 lysozyme mutants: implications for the interpretation of EPR spectra in terms of structure, Biochemistry 39 (2000) 8396–8405.
[15] J.P. Barnes, Z. Liang, H.S. Machaourab, J.H. Freed, W.L. Hubbell, A multifrequency electron spin resonance study of T4 Lysozyme dynamics, Biophys. J. 76 (1999) 3298–3306.
[16] D.E. Budil, S. Lee, S. Saxena, J.H. Freed, Nonlinear-least-squares analysis of slow-motion EPR spectra in one and two dimensions using a modified Levenberg-Marquardt algorithm, J. Mag. Res. A 120 (1996) 155–189.
[17] H.-J. Steinhoff, W.L. Hubbell, Calculation of electron paramagnetic resonance spectra from Brownian dynamics trajectories: application to nitroxide side chains in proteins, Biophys. J. 71 (1996) 2201–2212.
[18] H.-J. Steinhoff, A. Savitsky, C. Wegener, M. Pfeiffer, M. Plato, K. Mobius, High-field EPR studies of the structure and conformational changes of site-directed spin labelled bacteriorhodopsin, Biochim. Biophys. Acta 1457 (2000) 253–262.
[19] M.G. Finiguerra, I.M.C. Van Amsterdam, S. Alagaratnam, M. Ubbink, M. Huber, Anisotropic spin label mobilities in azurin from 95 GHz electron paramagnetic resonance spectroscopy, Chem. Phys. Lett. 382 (2003) 528–533.
[20] M. Bennati, G.J. Gerfen, G.V. Martinez, R.G. Griffiths, D.J. Singel, G.L. Millhauser, Nitroxide side chain dynamics in a spin labelled helix forming peptide revealed by high frequency (139.5 GHz) EPR spectroscopy, J. Mag. Res. 139 (1999) 281–286.
[21] H.S. Mchaourab, M.A. Lietzow, K. Hideg, W.L. Hubbell, Motion of spin-labelled side chains in T4 Lysozyme. Correlation with protein structure and dynamics, Biochemistry 35 (1996) 7692–7704.
[22] U.C. Kuhlmann, A.J. Pommer, G.R. Moore, R. James, C. Kleanthous, Specificity in protein–protein interactions: the structural basis for dual recognition in endonuclease colicin-immunity protein complexes, J. Mol. Biol. 301 (2000) 1163–1176.
[23] M.J. Osborne, A.L. Breeze, L.-Y. Lian, A. Reilly, R. James, C. Kleanthous, G.R. Moore, Three-dimensional solution structure and $^{13}C$ nuclear magnetic resonance assignments of the colicin E9 immunity protein Im9, Biochemistry 35 (1996) 9505–9512.
[24] R. James, C.N. Penfold, G.R. Moore, C. Kleanthous, Killing of *E. coli* cells by E group nuclease colicins, Biochimie 84 (2002) 381–389.
[25] R. Wallis, A. Reilly, A. Barnes, C. Abell, D.G. Cambell, G.R. Moore, R. James, C. Kleanthous, Tandem overproduction and characterisation of the nuclease domain of colicin E9 and its cognate inhibitor protein Im9, Eur. J. Biochem. 220 (1994) 447–454.
[26] C. Kleanthous, D. Walker, Immunity proteins: Enzyme inhibitors that avoid the active site, Trends Biochem. Sci. 26 (2001) 624–631.
[27] R. James, C. Kleanthous, G.R. Moore, The biology of E colicins: paradigms and paradoxes, Microbiology 142 (1996) 1569–1580.
[28] R. Wallis, G.R. Moore, R. James, C. Kleanthous, Protein–protein interactions in colicin E9 DNase-immunity protein complexes. 1. Diffusion controlled association and femtomolar binding for the cognate complex, Biochemistry 34 (1995) 13743–13750.
[29] C. Garinot-Schneider, A.J. Pommer, G.R. Moore, C. Kleanthous, R. James, Identification of putative active-site residues in the DNase domain of colicin E9 by random mutagenesis, J. Mol. Biol. 260 (1996) 731–742.
[30] W. Li, C.A. Dennis, G.R. Moore, R. James, C. Kleanthous, Protein–protein interaction specificity of Im9 for the endonuclease toxin colicin E9 defined by homolgue-scanning mutagenesis, J. Biol. Chem. 272 (1997) 22253–22258.
[31] P. Carl, 2003. The ER4123D CW-resonator: dedicated to spin labels, in: Bruker Biospin Application Note.

[32] W.L. Hubbell, W. Froncisz, J.S. Hyde, Continuous and stopped flow EPR spectrometer based on a loop gap resonator, Rev. Sci. Instrum. 58 (1987) 1879–1886.
[33] L.J. Schwartz, A.E. Stillman, J.H. Freed, Analysis of electron spin echoes by spectral representation of the stochastic Liouville equation, J. Chem. Phys. 77 (1982) 5410–5425.
[34] B.H. Robinson, L.J. Slutsky, F.P. Auteri, Direct simulation of continuous wave electron paramagnetic resonance spectra from Brownian dynamics trajectories, J. Chem. Phys. 96 (1992) 2609–2616.
[35] M. Ge, J.H. Freed, Electron spin resonance study of aggregation of gramicidin in dipalmoylphosphatidylcholine bilayers and hydrophobic mismatch, Biophys. J. 76 (1999) 264–280.
[36] Z. Liang, J.H. Freed, R.S. Keyes, A.M. Borbat, An electron spin resonance model of DNA dynamics using the slowly relaxing local structure model, J. Phys. Chem. B 104 (2000) 5372–5381.
[37] K.A. Fichthorn, W.H. Weinberg, Theoretical foundation of dynamical Monte Carlo simulations, J. Chem. Phys. 95 (1991) 1090–1095.
[38] V.P. Timofeev, V.I. Tsetlin, Analysis of the mobility of protein side chains by spin label technique, Biophys. Struct. Mech. 10 (1983) 93–108.
[39] D.J.B. Hunter, V.S. Oganesyan, J.C. Salerno, C.S. Butler, W.J. Ingledew, A.J. Thomson, Angular dependences of perpendicular and parallel mode electron paramagnetic resonance of oxidized beef heart cytochrome c, Biophys. J. 78 (2000) 439.
[40] V.S. Oganesyan, C.S. Butler, N.J. Watmough, C. Greenwood, A.J. Thomson, M.R. Cheesman, Nature of the coupling between the high-spin Fe(III) heme and Cu-B(II) in the active site of terminal oxidases: dual-mode EPR spectra of fluoride cytochrome bo3, J. Am. Chem. Soc. 120 (1998) 4232.
[41] E.T.J. Van Den Bremer, A.H. Keeble, A.J.W.G. Visser, A. Van Hoek, C. Kleanthous, A.J.R. Heck, W. Jiskoot, Ligand-induced changes in the conformational dynamics of a bacterial cytotoxic endonuclease, Biochemistry 43 (2004) 4347–4355.
[42] B.J. Gaffney, D. Marsh, High-frequency, spin-label EPR of nonaxial lipid ordering and motion in cholesterol-containing membranes, Proc. Natl. Acad. Sci. USA 95 (1998) 12940–12943.
[43] E.S. Collins, 2001. University of East Anglia, Norwich.
[44] S.B.M. Whittaker, M. Czisch, R. Wechselberger, R. Kaptein, A.M. Hemmings, R. James, C. Kleanthous, G.R. Moore, Slow conformational dynamics of an endonuclease persist in its complex with its natural protein inhibitor, Protein Sci. 9 (2000) 713–720.